

## SYNTHESES, CRYSTAL STRUCTURES, AND ANTIMICROBIAL ACTIVITIES OF ZINC COMPLEXES DERIVED FROM 2-AMINO-*N'*- (PYRIDIN-2-YLMETHYLENE)BENZOHYDRAZIDE

L. Zhang<sup>1</sup>, X. Feng<sup>1</sup>, Y. Gu<sup>1</sup>, T. Yang<sup>2</sup>, X. Li<sup>3</sup>,  
H. Yu<sup>1</sup>, and Z. You<sup>1\*</sup>

New zinc complexes, [ZnBr<sub>2</sub>(HL)] (**1**), [ZnBr(HL)(NCS)]·0.5H<sub>2</sub>O (**2**), [Zn(HL)L<sub>2</sub>] (**3**), and [ZnL<sub>2</sub>] (**4**), where L is the monoanionic form of 2-amino-*N'*-(pyridin-2-ylmethylene)benzohydrazide (HL), have been prepared and characterized by elemental analysis, IR and UV-Vis spectra, as well as single crystal X-ray diffraction. The Zn atoms in complexes **1-3** are in distorted trigonal-bipyramidal coordination, and that in complex **4** is in octahedral coordination. The crystal structures of the complexes are stabilized by hydrogen bonds. The antibacterial and antifungal activities of the compounds were evaluated.

**DOI:** 10.1134/S0022476622080170

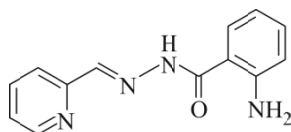
**Keywords:** hydrazone, zinc complex, crystal structure, antimicrobial activity.

### INTRODUCTION

Hydrazones and their derivatives are a special type of Schiff bases, which have interesting and fascinating pharmaceutical and biological activities like antibacterial, antifungal, anti-inflammatory, antiviral and antitumor [1-4]. Metal complexes derived from hydrazone ligands are important in bioinorganic chemistry [5-11]. In particular, when coordinated to transition metals, they significantly expand the lipophilic character that contributes to increasing potential biological complexes [12]. In order to obtain metal complexes, it is necessary to use active metals that have low toxicity to organisms [13]. Zinc complexes with hydrazone ligands have shown various biological activities [14-17]. In the past few years, a number of zinc complexes with hydrazone ligands have been reported for their synthesis, crystal structures and biological application. The coordination geometries of zinc complexes are usually tetrahedral, square pyramidal, trigonal bipyramidal and octahedral [18-23]. The hydrazones adopt either ketone or enol form during the coordination. However, it is hard to predict which form they will present. As a continuation of our work on the hydrazone complexes [24-26], and to control the coordination mode of hydrazone ligands, as well as in pursuit of new biological agents, we reported here a series of new zinc complexes, [ZnBr<sub>2</sub>(HL)] (**1**), [ZnBr(HL)(NCS)]·0.5H<sub>2</sub>O (**2**), [Zn(HL)L<sub>2</sub>] (**3**) and [ZnL<sub>2</sub>] (**4**), where HL is 2-amino-*N'*-(pyridin-2-ylmethylene)benzohydrazide (Scheme 1).

---

<sup>1</sup>Department of Chemistry and Chemical Engineering, Liaoning Normal University, Dalian, People's Republic of China; \*youzhonglu@163.com. <sup>2</sup>Dalian Institute of Chemical Physics, Chinese Academy of Sciences, Dalian, People's Republic of China. <sup>3</sup>Zibo Vocational Institute, Zibo, People's Republic of China. Original article submitted February 21, 2022; revised March 31, 2022; accepted March 31, 2022.



Scheme 1. HL.

## EXPERIMENTAL

**Materials and measurements.** The starting materials 2-pyridinecarboxaldehyde and 2-aminobenzohydrazide (AR grade) were purchased from Bailingwei Chemicals Co. Ltd. of China. Zinc chloride, zinc bromide, zinc iodide, zinc acetate, ammonium thiocyanate and solvents with AR grade were purchased from Xiya Chemicals Co. Ltd. of China. The ligand HL was prepared according to the literature method [27]. CHN elemental analyses were performed on a PerkinElmer 240C elemental analyzer. IR spectra were recorded on a Jasco FTIR-4000 spectrometer as KBr pellets in the 4000–400  $\text{cm}^{-1}$  region. UV-Vis spectra were recorded on a LAMBDA 35 spectrometer. Single crystal X-ray diffraction was carried out on a Bruker SMART 1000 CCD diffractometer.

**Synthesis of [ZnBr<sub>2</sub>(HL)] (1).** To a 15 mL methanolic solution of HL (0.24 g, 1.0 mmol) a methanolic solution (15 mL) of zinc bromide (0.26 g, 1.0 mmol) was added slowly. The mixture was stirred for 30 min and filtered. The colorless solution was left undisturbed in air for slow evaporation. After 5 days colorless single crystals of the complex that separated, were washed with cold methanol and dried *in vacuo* over silica gel indicator. Yield: 0.22 g (47%). Anal. calcd for C<sub>13</sub>H<sub>11</sub>Br<sub>2</sub>N<sub>4</sub>OZn (%): C 33.62; H 2.39; N 12.06. Found (%): C 33.41; H 2.50; N 11.87. IR data ( $\text{cm}^{-1}$ ): 3473, 3358 (NH<sub>2</sub>), 3210 (NH), 1632 (C=N), 1577, 1552, 1522, 1471, 1446, 1357, 1285, 1247, 1162, 937, 776, 742, 534, 492. UV-Vis data (nm, L/(mol·cm)): 306,  $6.72 \cdot 10^3$ ; 325,  $4.51 \cdot 10^3$ ; 380,  $1.72 \cdot 10^3$ .

**Synthesis of [ZnBr(HL)(NCS)]·0.5H<sub>2</sub>O (2).** To a 15 mL methanolic solution of HL (0.24 g, 1.0 mmol) and ammonium thiocyanate (0.076 g, 1.0 mmol) a methanolic solution (15 mL) of zinc bromide (0.26 g, 1.0 mmol) was added slowly. The mixture was stirred for 30 min and filtered. The colorless solution was left undisturbed in air for slow evaporation. After 5 days colorless single crystals of the complex that separated, were washed with cold methanol and dried *in vacuo* over silica gel indicator. Yield: 0.31 g (67%). Anal. calcd for C<sub>14</sub>H<sub>13</sub>BrN<sub>5</sub>O<sub>1.5</sub>SZn (%): C 37.15; H 2.89; N 15.47. Found (%): C 36.86; H 3.07; N 15.32. IR data ( $\text{cm}^{-1}$ ): 3477, 3359 (NH<sub>2</sub>), 3210 (NH), 2088 (NCS), 1633 (C=N), 1580, 1551, 1521, 1463, 1442, 1399, 1355, 1328, 1290, 1276, 1245, 1163, 1102, 935, 775, 739, 696, 669, 530. UV-Vis data (nm, L/(mol·cm)): 239,  $5.59 \cdot 10^3$ ; 325,  $2.87 \cdot 10^3$ ; 390,  $3.13 \cdot 10^3$ .

**Synthesis of [Zn(HL)I<sub>2</sub>] (3).** Complex 3 was prepared by metathesis of complex 1, with zinc bromide replaced by zinc iodide (0.32 g, 1.0 mmol). Yield: 0.35 g (62%). Anal. calcd for C<sub>13</sub>H<sub>12</sub>I<sub>2</sub>N<sub>4</sub>OZn (%): C 27.91; H 2.16; N 10.01. Found (%): C 28.16; H 2.25; N 9.89. IR data ( $\text{cm}^{-1}$ ): 3468, 3358 (NH<sub>2</sub>), 3214 (NH), 1632 (C=N), 1581, 1547, 1518, 1471, 1446, 1352, 1327, 1298, 1247, 1158, 1102, 928, 780, 742, 670, 526, 492. UV-Vis data (nm, L/(mol·cm)): 303,  $6.81 \cdot 10^3$ ; 325,  $4.32 \cdot 10^3$ ; 368,  $3.87 \cdot 10^3$ .

**Synthesis of [ZnL<sub>2</sub>] (4).** To a 15 mL methanolic solution of HL (0.24 g, 1.0 mmol) and 2,2'-bipyridine (0.016 g, 1.0 mmol) a methanolic solution (15 mL) of zinc bromide (0.26 g, 1.0 mmol) was added slowly. The mixture was stirred for 30 min and filtered. The colorless solution was left undisturbed in air for slow evaporation. After 5 days colorless single crystals of the complex that separated, were washed with cold methanol and dried *in vacuo* over silica gel indicator. Yield: 0.25 g (46%). Anal. calcd for C<sub>26</sub>H<sub>22</sub>N<sub>8</sub>O<sub>2</sub>Zn (%): C 36.58; H 2.63; N 15.24. Found (%): C 36.71; H 2.55; N 15.05. IR data ( $\text{cm}^{-1}$ ): 3451, 3392 (NH<sub>2</sub>), 3277 (NH), 1603 (C=N), 1561, 1488, 1463, 1445, 1340, 1285, 1251, 1145, 1073, 920, 759, 687, 632, 593, 539, 462. UV-Vis data (nm, L/(mol·cm)): 238,  $5.35 \cdot 10^3$ ; 295,  $3.87 \cdot 10^3$ ; 383,  $5.56 \cdot 10^3$ .

**X-ray diffraction.** Diffraction intensities for the complexes were collected at 298(2) K using a Bruker SMART 1000 CCD area-detector diffractometer with MoK<sub>α</sub> radiation ( $\lambda = 0.71073 \text{ \AA}$ ). The collected data were reduced with the

SAINT [28], and multi-scan absorption correction was performed using the SADABS [29]. The structures of the complexes were solved by direct method and refined against  $F^2$  by full-matrix least-squares method using the SHELXL-2018/3 package [30]. All of the non-hydrogen atoms were refined anisotropically. The amino H atoms were located from difference Fourier maps and refined isotropically, with N–H and H···H distances restrained to 0.90(1) Å and 1.45(2) Å, respectively. The water H atoms were located from difference Fourier maps and refined isotropically, with O–H and H···H distances restrained to 0.96(1) Å and 1.47(2) Å, respectively. The remaining hydrogen atoms were placed in calculated positions and constrained to ride on their parent atoms. There is no acceptor for O3–H3A and O3–H3B bonds in complex **2**, which is due to the disorder of the water molecule, and it is difficult to add the hydrogen atoms at the right positions. The crystallographic data for the complexes are summarized in Table 1. Selected bond lengths and angles are given in Tables 2 and 3.

**Antimicrobial assay.** The antibacterial activities of the compounds were tested against *B. subtilis*, *S. aureus*, *E. coli*, and *P. fluorescens* using MH (Mueller–Hinton) medium. The antifungal activities of the compounds were tested against *C. albicans* and *A. niger* using RPMI-1640 medium. The MIC values of the tested compounds were determined by a colorimetric method using the dye MTT [31]. A stock solution of the aroylhydrazone compound (150 µM) in DMSO was prepared and graded quantities (75 µM, 37.5 µM, 18.8 µM, 9.4 µM, 4.7 µM, 2.3 µM, 1.2 µM, 0.59 µM) of the tested compounds were incorporated in specified quantity of the corresponding sterilized liquid medium. A specified quantity of the medium containing the compound was poured into microtitration plates. Suspension of the microorganism was prepared to contain approximately  $10^5$  cfu/mL and applied to microtitration plates with serially diluted compounds in DMSO to be tested and incubated at 37 °C for 24 h and 48 h for bacteria and fungi, respectively. Then the MIC values were visually determined on each of the microtitration plates, 50 µL of PBS (phosphate buffered saline 0.01 M, pH = 7.4) containing 2 mg of MTT/mL

**TABLE 1.** Crystallographic and Experimental Data for the Complexes

Compound	<b>1</b>	<b>2</b>	<b>3</b>	<b>4</b>
Formula	C <sub>13</sub> H <sub>12</sub> Br <sub>2</sub> N <sub>4</sub> OZn	C <sub>14</sub> H <sub>13</sub> BrN <sub>5</sub> O <sub>1.5</sub> SZn	C <sub>13</sub> H <sub>12</sub> I <sub>2</sub> N <sub>4</sub> OZn	C <sub>26</sub> H <sub>22</sub> N <sub>8</sub> O <sub>2</sub> Zn
Formula weight	465.46	452.63	559.44	543.88
Crystal shape / color	Block / colorless	Block / colorless	Block / colorless	Block / colorless
Crystal size, mm	0.20×0.18×0.17	0.18×0.17×0.17	0.18×0.15×0.15	0.33×0.30×0.28
Crystal system	Monoclinic	Monoclinic	Monoclinic	Monoclinic
Space group	<i>P</i> 2 <sub>1</sub> / <i>c</i>	<i>P</i> 2 <sub>1</sub> / <i>c</i>	<i>P</i> 2 <sub>1</sub> / <i>c</i>	<i>P</i> 2 <sub>1</sub> / <i>n</i>
<i>a</i> , <i>b</i> , <i>c</i> , Å	13.7533(13), 14.7742(18), 7.6164(11)	8.5250(10), 13.1640(13), 16.5270(15)	13.6455(17), 15.679(2), 7.9227(11)	8.806(2), 13.5800(11), 20.6453(18)
β, deg	95.676(2)	96.646(2)	95.229(2)	97.871(2)
<i>V</i> , Å <sup>3</sup>	1540.0(3)	1842.2(3)	1688.0(4)	2445.5(6)
<i>Z</i>	4	4	4	4
<i>D</i> <sub>c</sub> , g/cm <sup>3</sup>	2.008	1.632	2.201	1.477
μ, mm <sup>-1</sup>	6.786	3.628	5.115	1.046
<i>F</i> (000)	904	900	1048	1120
θ range, deg	1.49 / 25.50	1.98 / 25.50	1.50 / 25.50	1.80 / 25.49
Reflections / parameters	8913 / 199	9008 / 223	9870 / 199	14339 / 350
Unique / observed reflections ( <i>I</i> ≥ 2σ( <i>I</i> ))	2851 / 2321	3323 / 1449	3145 / 2446	4549 / 3386
Restraints	4	3	4	6
<i>GOOF</i> on <i>F</i> <sup>2</sup>	1.080	1.012	1.025	1.045
<i>R</i> <sub>1</sub> , <i>wR</i> <sub>2</sub> ( <i>I</i> ≥ 2σ( <i>I</i> )) <sup>#1</sup>	0.0406, 0.1104	0.0899, 0.2316	0.0351, 0.0808	0.0382, 0.0862
<i>R</i> <sub>1</sub> , <i>wR</i> <sub>2</sub> (all data)	0.0528, 0.1176	0.1934, 0.3027	0.0517, 0.0891	0.0589, 0.0944

<sup>#1</sup>  $R_1 = \sum ||F_0| - |F_c|| / \sum |F_0|$ ,  $wR_2 = [\sum w(F_0^2 - F_c^2)^2 / \sum w(F_0^2)^2]^{1/2}$ .

**TABLE 2.** Selected Bond Lengths (Å) and Angles (deg) for Complexes 1-3

Bond length	1	2	3
Zn1–N1	2.204(5)	2.184(9)	2.205(5)
Zn1–N2	2.098(4)	2.084(9)	2.107(4)
Zn1–O1	2.262(4)	2.212(8)	2.269(4)
Zn1–X1	2.3447(9)	2.419(2)	2.5381(8)
Zn1–X2	2.3882(9)		2.5675(9)
Zn1–N5		1.932(13)	
Bond angles	1	2	3
N2–Zn1–N1	74.30(16)	74.9(4)	74.10(16)
N2–Zn1–O1	71.14(15)	73.1(4)	71.13(15)
N1–Zn1–O1	145.26(15)	147.9(4)	144.93(16)
N2–Zn1–Br1	129.47(13)	132.0(2)	130.57(13)
N1–Zn1–Br1	102.20(13)	100.1(3)	103.84(12)
O1–Zn1–Br1	96.94(11)	98.7(3)	95.33(11)
N2–Zn1–Br2	114.67(13)		114.44(13)
N1–Zn1–Br2	100.06(13)		99.84(13)
O1–Zn1–Br2	97.40(12)		98.44(12)
Br1–Zn1–Br2	115.52(3)		114.51(3)
N5–Zn1–N2		113.5(5)	
N5–Zn1–N1		100.0(4)	
N5–Zn1–O1		95.6(4)	
N5–Zn1–Br1		114.4(4)	

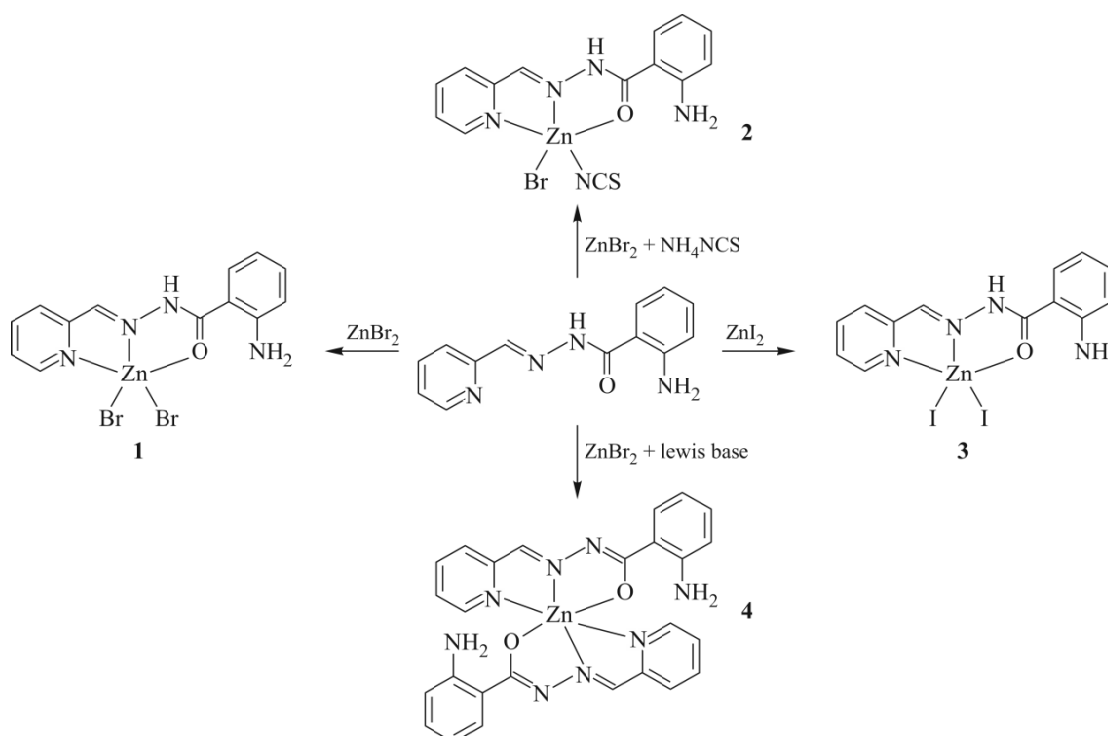
**TABLE 3.** Selected Bond Lengths (Å) and Angles (deg) for Complex 4

Bond length	Distance	Bond length	Distance
Zn1–O1	2.0758(18)	Zn1–O2	2.1566(18)
Zn1–N1	2.227(2)	Zn1–N2	2.060(2)
Zn1–N5	2.257(2)	Zn1–N6	2.040(2)
Bond angle	Value	Bond angle	Value
N6–Zn1–N2	175.37(8)	N6–Zn1–O1	109.41(8)
N2–Zn1–O1	74.85(7)	N6–Zn1–O2	73.96(8)
N2–Zn1–O2	107.61(8)	O1–Zn1–O2	97.82(7)
N6–Zn1–N1	100.32(8)	N2–Zn1–N1	75.33(8)
O1–Zn1–N1	150.10(8)	O2–Zn1–N1	93.23(7)
N6–Zn1–N5	75.66(9)	N2–Zn1–N5	102.35(9)
O1–Zn1–N5	96.21(8)	O2–Zn1–N5	149.31(8)
N1–Zn1–N5	87.94(8)		

was added to each well. Incubation was continued at room temperature for 4-5 h. The content of each well was removed, and 100  $\mu$ L of isopropanol containing 5% 1 M HCl was added to extract the dye. After 12 h of incubation at room temperature, the optical density was measured with a microplate reader at 550 nm.

## RESULTS AND DISCUSSION

**Chemistry.** The hydrazone HL was facial prepared by the reaction of 2-pyridinecarboxaldehyde and 2-aminobenzohydrazide with 1:1 molar ratio in methanol. The zinc complexes **1-3** with tetrahedral coordination were synthesized from the reaction of HL with zinc bromide, zinc bromide and ammonium thiocyanate, and zinc iodide, respectively in methanol. The zinc complex **4** with octahedral coordination was synthesized from the reaction of HL with zinc bromide in the presence of 2,2'-bipyridine (Scheme 2). Interestingly, when 2,2'-bipyridine was replaced by other Lewis bases like 4,4'-bipyridine, pyridine, or 1,10-phenanthroline, the same structures as complex **4** can be obtained. Thus, the presence of Lewis bases contributes to the enol form of the hydrazone compound. While no Lewis bases, the hydrazone presents in ketone form. All the complexes are soluble in methanol and ethanol. Single crystals of the complexes were obtained by slow evaporation of the methanolic solution of the complexes. The crystals of the complexes are stable in air at room temperature.



**Scheme 2.** The synthetic procedure of the complexes.

The coordination of HL to Zn cation affects the bond lengths with adjacent atoms in the structure of organic ligand when compared with the structure of individual HL. In complexes **1-3**, the ligands are in neutral ketone form. The C6=N2 bond length in HL is shorter than those in complexes **1** and **2**, and comparable to that in complex **3**. The N2–N3 bond length in HL is longer than those in complexes **1-3**. The C7–N3 bond length in HL is shorter than those in complexes **1** and **3**, and longer than that in complex **2**. The C7–O1 bond length in HL is shorter than those in complexes **2** and **3**, and comparable to that in complex **1**. While in complex **4**, the ligands are in monoanionic enolate form. The C6=N2 and C7–O1 bond lengths in HL are shorter than those in complex **4**. The N2–N3 and C7–N3 bond lengths in HL are longer than those in complex **4**.

**Structure description of complexes 1-3.** The molecular structures of complexes **1-3** are shown in Figs. 1-3, respectively. The complexes crystallize in the monoclinic space group  $P2_1/c$ . The Zn atom in each complex is in distorted trigonal-bipyramidal coordination, with the equatorial plane defined by the imino nitrogen (N2) of the hydrazone ligand, and two halide or pseudohalide ligands, *viz.* Br1 and Br2 for **1**, Br1 and N5 for **2**, and I1 and I2 for **3**, and with the axial positions

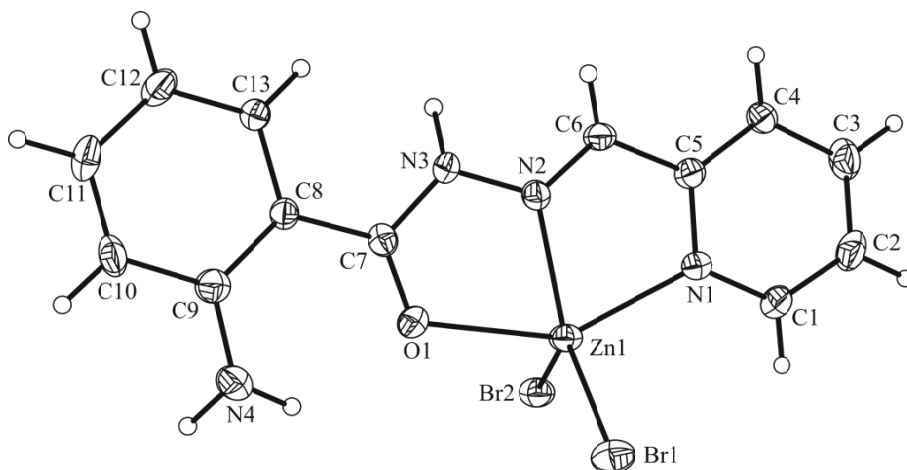


**Fig. 1.** Molecular structure of complex **1** with the atom labeling scheme. Thermal ellipsoids are drawn at the 30% probability level.

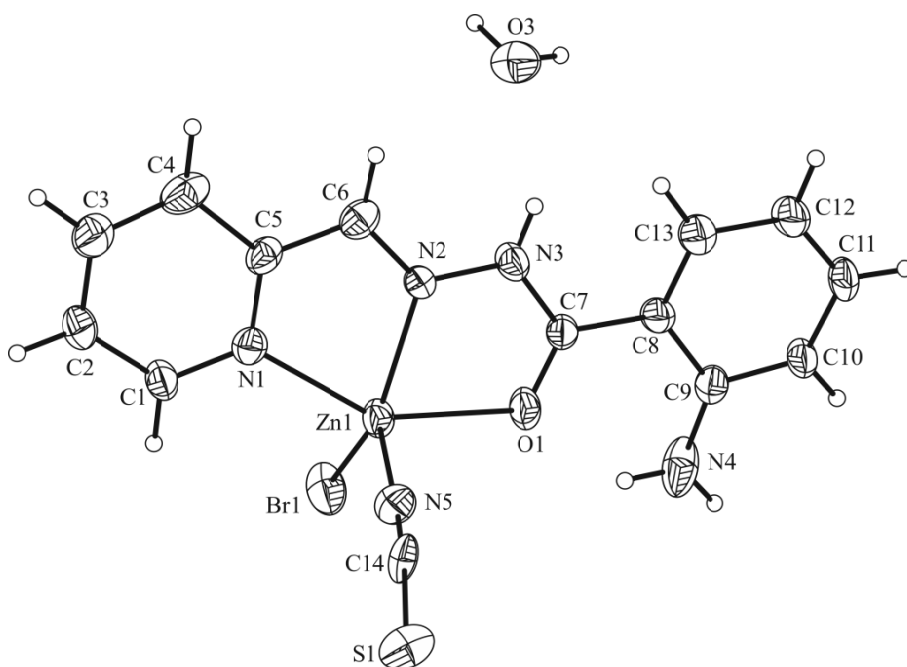


**Fig. 2.** Molecular structure of complex **2** with the atom labeling scheme. Thermal ellipsoids are drawn at the 30% probability level.

occupied by the pyridine nitrogen (N1) and carbonyl oxygen (O1) atoms of the hydrazone ligand. The Zn–O and Zn–N bond lengths in the complexes are similar, and are comparable to those observed in zinc complexes with hydrazone ligands [32–37]. The trigonal-bipyramidal coordination in each complex is distorted from ideal geometry, as indicated by the bond lengths and angles. The equatorial bond angles of 114.67(13)–129.47(13)° for **1**, 114.4(4)–132.0(2)° for **2**, and 114.44(13)–130.57(13)° for **3**, as well as the angles among the axial and equatorial donor atoms of 71.14(15)–102.22(13)° for **1**, 73.1(4)–100.1(3)° for **2**, and 71.13(15)–103.84(12)° for **3**, indicate the distortion of the trigonal-bipyramidal coordination. The distortion can be further observed from the perpendicular angles between the two axial bonds of 145.25(15)° for **1**, 147.9(4)° for **2**, and 144.93(16)° for **3**.

The pyridine ring and the benzene ring form a dihedral angle of 6.2(4)° for **1**, 5.7(4)° for **2**, and 7.5(5)° for **3**. The dihedral angle between the benzene ring and the ring C8–C9–N4–H4B⋯O1–C7 is 1.2(4)° for **1**, 5.4(4)° for **2**, and 3.9(5)° for **3**.

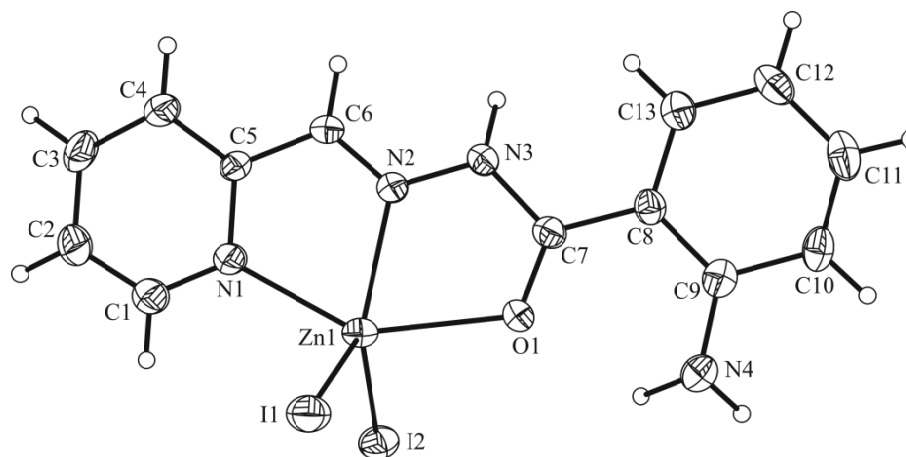


**Fig. 3.** Molecular structure of complex **3** with the atom labeling scheme. Thermal ellipsoids are drawn at the 30% probability level.

**3**, indicating they are approximately coplanar. This is caused by the presence of N4–H4B···O1 hydrogen bond. In the crystal structure of complex **1**, the molecules are linked through N–H···Br hydrogen bonds (Table 4), to form two-dimensional network along the *bc* plane (Fig. 4). In the crystal structure of complex **2**, the complex molecules are linked by water molecules through N–H···O and O–H···Br hydrogen bonds (Table 4), to form one-dimensional chains along the *b* axis. The amino H atom forms an intramolecular N–H···O hydrogen bond (Fig. 5). In the crystal structure of complex **3**, the molecules are linked through N–H···I hydrogen bonds (Table 4), to form two-dimensional network along the *ab* plane (Fig. 6).

**TABLE 4.** Hydrogen Bond Distances (Å) and Bond Angles (deg) for the Complexes

<i>D</i> –H··· <i>A</i>	<i>d</i> ( <i>D</i> –H)	<i>d</i> (H··· <i>A</i> )	<i>d</i> ( <i>D</i> ··· <i>A</i> )	∠( <i>D</i> –H··· <i>A</i> )
<b>1</b>				
N3–H3···Br2 <sup>#1</sup>	0.90(1)	2.67(6)	3.346(5)	133(7)
N4–H4A···Br2 <sup>#2</sup>	0.90(1)	2.92(5)	3.653(5)	140(6)
N4–H4B···O1	0.90(1)	2.08(5)	2.675(7)	123(5)
<b>2</b>				
O3–H3A···Br1 <sup>#3</sup>	0.96(1)	3.0(2)	3.413(14)	111(15)
O3–H3A···S1 <sup>#4</sup>	0.96(1)	2.99(19)	3.702(17)	132(19)
N3–H3···O3	0.86	2.18	2.934(17)	146(11)
N4–H4B···O1	0.86	2.08	2.699(15)	128(11)
<b>3</b>				
N3–H3···I2 <sup>#5</sup>	0.90(1)	2.73(3)	3.572(5)	156(6)
N4–H4B···O1	0.90(1)	2.07(5)	2.656(7)	122(5)
N4–H4A···I2 <sup>#6</sup>	0.90(1)	3.00(2)	3.861(6)	161(5)
<b>4</b>				
N8–H8A···N7	0.88(1)	2.06(2)	2.674(4)	125(2)
N4–H4B···O2 <sup>#7</sup>	0.88(1)	2.247(11)	3.107(3)	166(2)
N4–H4A···N3	0.89(1)	2.064(17)	2.726(3)	130(2)

Symmetry codes: <sup>#1</sup> *x*, 1/2–*y*, –1/2+*z*; <sup>#2</sup> –*x*, 1–*y*, 1–*z*; <sup>#3</sup> 1–*x*, –1/2+*y*, 1/2–*z*; <sup>#4</sup> 1–*x*, –*y*, 1–*z*; <sup>#5</sup> *x*, 3/2–*y*, 1/2+*z*; <sup>#6</sup> 1–*x*, 2–*y*, 1–*z*; <sup>#7</sup> 1–*x*, 1–*y*, 1–*z*.

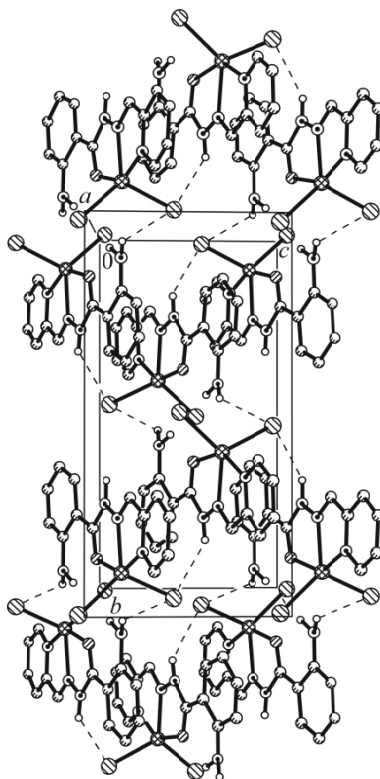


**Fig. 4.** Molecular packing diagram of complex **1**. Hydrogen bonds are shown as dashed lines. The hydrogen atoms not involved in the formation of hydrogen bonds are omitted for clarity.

**Structure description of complex 4.** The molecular structure complex **4** is shown in Fig. 7. The complex crystallizes in the monoclinic space group  $P2_1/n$ . The Zn atom in the complex is in octahedral coordination, with the equatorial plane defined by the pyridine nitrogen (N1), imino nitrogen (N2) and enolate oxygen (O1) and the other imino nitrogen (N6) from two hydrazone ligands, and with the two axial positions occupied by the pyridine nitrogen (N5) and enolate oxygen (O2) of the hydrazone ligand. The octahedral coordination is distorted from octahedral geometry, as indicated by the bond lengths and angles. The Zn–O and Zn–N bond lengths in the complex are 2.0758(18)-2.1566(18) Å and 2.040(2)-2.257(2) Å, respectively, which are comparable to those observed in zinc complexes with hydrazone ligands [38-42]. The *cis* and *trans* coordinate bond angles are 73.96(8)-109.41(8)° and 149.31(8)-175.37(8)°, indicate the distortion of the octahedral coordination.

The pyridine ring and the benzene ring form a dihedral angle of 7.3(4)° for one hydrazone ligand, and 22.7(5)° for the other one. The dihedral angle between the C8–C13 benzene ring and the ring C8–C13–N4–H4A···N3–C7 is 1.1(4)°, and that between the C21–C26 benzene ring and the ring C21–C22–N8–H8A···N7–C20 is 1.8(4)°. There present N4–H4A···N3 and N8–H8A···N7 hydrogen bonds in the ligands. In the crystal structure of the complex, the molecules are linked through N–H···O hydrogen bonds (Table 4), to form two-dimensional network along the *bc* plane (Fig. 8).

**IR and UV spectra.** The IR spectra of the free hydrazone and the complexes were recorded in the region of 4000-400  $\text{cm}^{-1}$  using KBr pellets. The infrared absorption bands at 3482  $\text{cm}^{-1}$  and 3373  $\text{cm}^{-1}$  are assigned to the stretching vibrations of  $\text{NH}_2$ , and that at 3205  $\text{cm}^{-1}$  is assigned to NH. The free hydrazone exhibits strong band at 1641  $\text{cm}^{-1}$  due to the C=O group, and the medium band at 1611  $\text{cm}^{-1}$  can be attributed to azomethine group,  $\mu(\text{C}=\text{N})$  [43]. In the complexes **1-3**, these bands are observed at 1632-1633  $\text{cm}^{-1}$  for the conjugated groups  $-\text{CH}=\text{N}-\text{N}=\text{C}(\text{O})-$ . While in the spectrum of complex



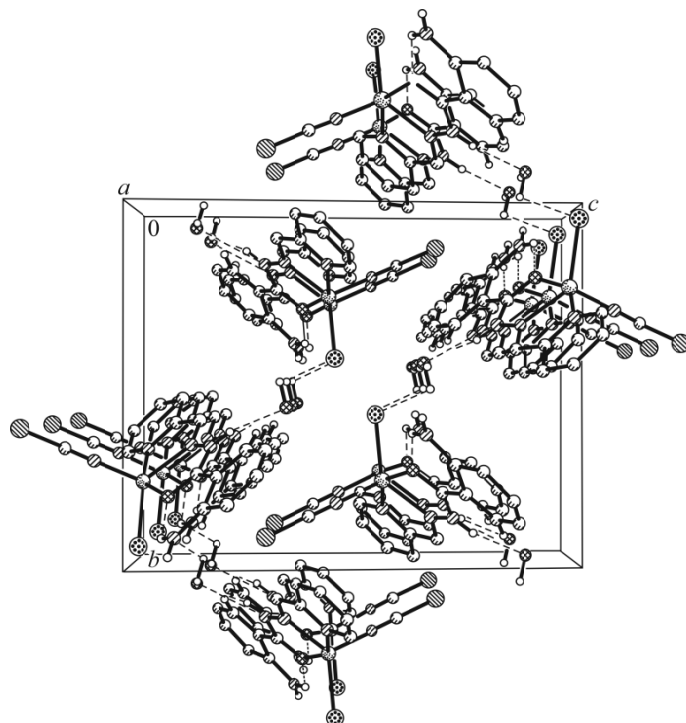


**Fig. 5.** Molecular packing diagram of complex **2**. Hydrogen bonds are shown as dashed lines. The hydrogen atoms not involved in the formation of hydrogen bonds are omitted for clarity.

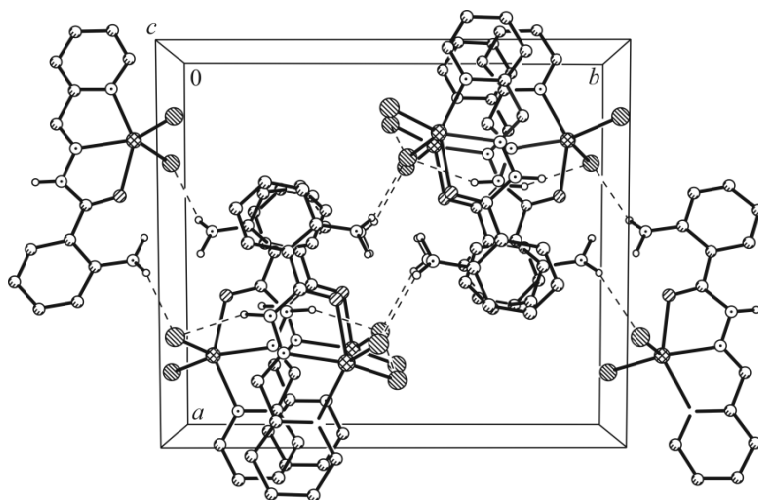


**Fig. 6.** Molecular packing diagram of complex **3**. Hydrogen bonds are shown as dashed lines. The hydrogen atoms not involved in the formation of hydrogen bonds are omitted for clarity.

**4**, the C=N vibration is located at  $1603\text{ cm}^{-1}$  [44]. The wave numbers of the azomethine groups in complexes **1**, **2** and **3** are located at higher frequencies, while that in complex **4** is located at lower frequency when compared with that of HL. This agrees with the different types of the hydrazone ligands, *viz.* ketone for **1**, **2** and **3**, and enol for **4**. The complexes show characteristic absorptions in the region  $3200\text{--}3500\text{ cm}^{-1}$  that can be assigned to NH stretching bands. In the spectrum of complex **2**, the intense and typical band at  $2088\text{ cm}^{-1}$  is assigned to the vibration of the thiocyanate ligand [45].

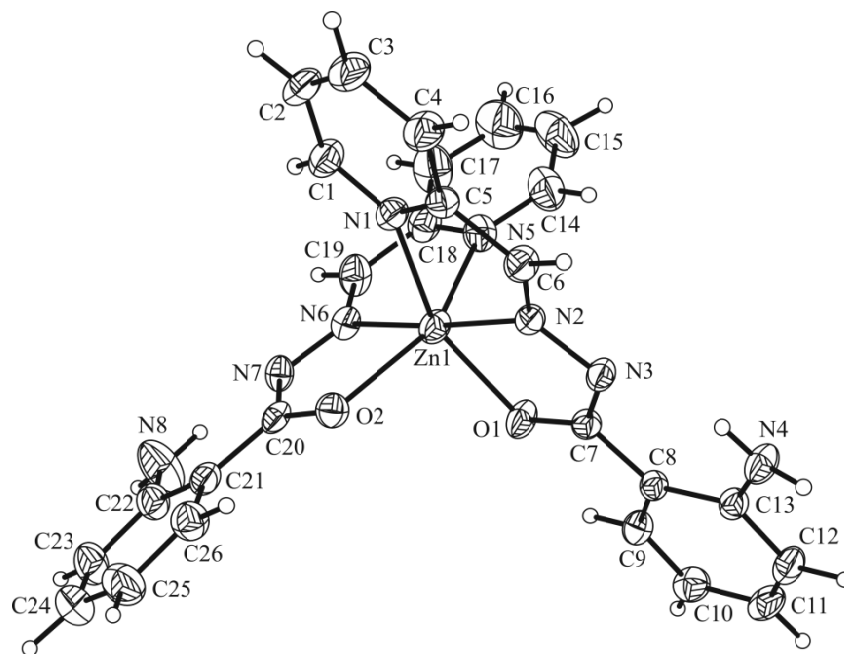


**Fig. 7.** Molecular structure of complex **4** with the atom labeling scheme. Thermal ellipsoids are drawn at the 30% probability level.

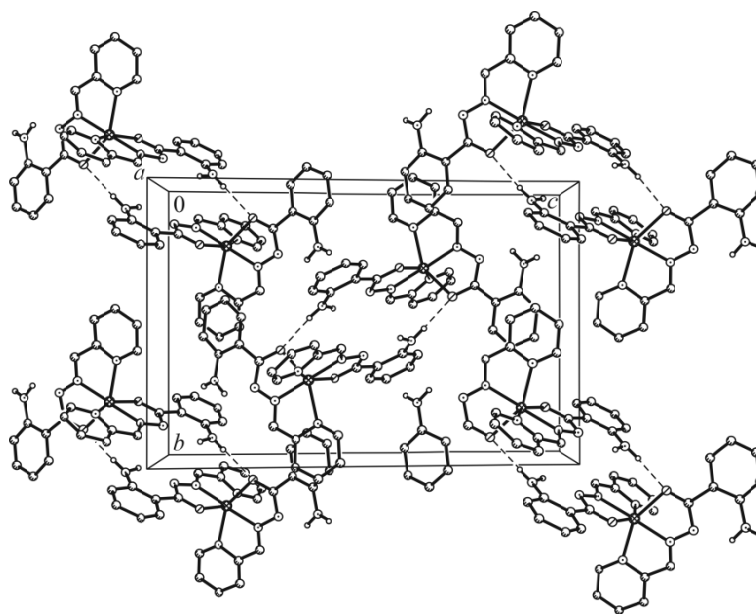


**Fig. 8.** Molecular packing diagram of complex **4**. Hydrogen bonds are shown as dashed lines. The hydrogen atoms not involved in the formation of hydrogen bonds are omitted for clarity.

The UV spectra of the hydrazone and the complexes were recorded in methanol. In the spectrum of the free hydrazone, the bands at 350 nm are attributed to the azomethine chromophore  $\pi-\pi^*$  transition. The bands at higher energies (300 nm) are associated with the benzene  $\pi-\pi^*$  transition. In the spectra of the complexes, the peaks in the region 295-325 nm can be assigned to intraligand transitions, and those in the region 360-390 nm may correspond to the ligand-to-metal charge transfer [46].

**Antimicrobial activity.** The hydrazone and the complexes were screened for antibacterial activity against two Gram (+) bacterial strains (*Bacillus subtilis* and *Staphylococcus aureus*) and two Gram (-) bacterial strains (*Escherichia coli*

**TABLE 5.** The MIC Values ( $\mu\text{M}$ ) of the Compounds

Tested material	<i>B. subtilis</i>	<i>S. aureus</i>	<i>E. coli</i>	<i>P. fluorescens</i>	<i>C. albicans</i>	<i>A. niger</i>
HL	9.4	37.5	37.5	>150	>150	>150
<b>1</b>	2.3	4.7	9.4	18.8	>150	>150
<b>2</b>	2.3	4.7	9.4	18.8	>150	>150
<b>3</b>	2.3	4.7	9.4	18.8	>150	>150
<b>4</b>	4.7	18.8	18.8	75	>150	>150
Kanamycin	0.6	2.3	4.7	4.7	>150	>150
Penicillin G	2.3	4.7	>150	>150	>150	>150
Ketoconazole	>150	>150	>150	>150	4.7	18.8

and *Pseudomonas fluorescens*) by MTT method. The MIC (minimum inhibitory concentration) values of the compounds against four bacteria are listed in Table 5. Kanamycin and Penicillin G were used as the standard agents. The free hydrazone has medium activity against *B. subtilis*, and weak activity against *S. aureus* and *E. coli*, while inactive against *P. fluorescens*. In general, the complexes have better activities against the bacteria than the free hydrazone. Interestingly, complexes **1-3** have similar activities against all the bacteria strains. Thus, the Br, NCS and I ligands have no obvious influence on the antibacterial activity. The three complexes showed strong activity against *B. subtilis* and *S. aureus*, medium activity against *E. coli*, and weak activity against *P. fluorescens*. Complex **4** showed good activity against *B. subtilis*, and weak activity against the remaining bacteria strains. Interestingly, complexes **1-3** have effective activity against *B. subtilis* and *S. aureus*, which are comparable to the reference drug Penicillin G.

The antifungal activity of the compounds was also evaluated against two fungal strains (*Candida albicans* and *Aspergillus niger*) by MTT method. Ketoconazole was used as a reference agent. Complexes **1-3** have weak activity against *P. fluorescens*, while no activity against *C. albicans* and *A. niger*. Complex **4** has very weak activity against *P. fluorescens*, which is weaker than complexes **1-3**.

## CONCLUSIONS

In summary, the present paper reports the synthesis, characterization and crystal structures of four new zinc complexes with the ligand 2-amino-*N'*-(pyridin-2-ylmethylene)benzohydrazide. The hydrazone ligand coordinates to the Zn atom through the pyridine nitrogen, imino nitrogen and carbonyl oxygen. When Lewis bases were added to the reaction mixture, the hydrazone ligand coordinates to the Zn atom through the pyridine nitrogen, imino nitrogen and enolate oxygen. Thus, the presence of Lewis bases contributes to the enolate form of the hydrazone compound. The complexes have effective antibacterial activity against *S. aureus*.

## ACKNOWLEDGMENTS

This work was financially supported by the high-level scientific research achievement funding program of Liaoning Normal University (grant number 21GDL003).

## ADDITIONAL INFORMATION

CCDC - 2116737 (**1**), 2116738 (**2**), 2116739 (**3**) and 2116740 (**4**) contain the supplementary crystallographic data for this article. These data can be obtained free of charge at <http://www.ccdc.cam.ac.uk/const/retrieving.html> or from the Cambridge Crystallographic Data Centre (CCDC), 12 Union Road, Cambridge CB2 1EZ, UK; Fax: +44(0)1223-336033 or E-mail: [deposit@ccdc.cam.ac.uk](mailto:deposit@ccdc.cam.ac.uk).

## CONFLICT OF INTERESTS

The authors declare that they have no conflicts of interests.

## REFERENCES

1. K. Pyta, A. Janas, M. Szukowska, P. Pecyna, M. Jaworska, M. Gajecka, F. Bartl, and P. Przybylski. *Eur. J. Med. Chem.*, **2019**, *167*, 96-104. <https://doi.org/10.1016/j.ejmech.2019.02.009>
2. I. Shabeeb, L. Al-Essa, M. Shtaiwi, E. Al-Shalabi, E. Younes, R. Okasha, and M. Abu Sini. *Lett. Org. Chem.*, **2019**, *16*, 430-436. <https://doi.org/10.2174/15701786166666181227122326>
3. Y. C. Wu, X. D. Ding, L. Ding, Y. S. Zhang, L. Cui, L. Sun, W. Li, D. Wang, and Y. F. Zhao. *Eur. J. Med. Chem.*, **2018**, *158*, 247-258. <https://doi.org/10.1016/j.ejmech.2018.09.004>
4. G.-X. He and L.-W. Xue. *Acta Chim. Slov.*, **2021**, *68*, 567-574. <https://doi.org/10.17344/acsi.2020.6333>
5. A. Thirugnanasundar, M. P. Kesavan, S. M. Kumar, L. Ravi, R. Bhaskar, G. Rajagopal, and J. Rajesh. *Inorg. Chim. Acta*, **2021**, *526*, 120543. <https://doi.org/10.1016/j.ica.2021.120543>
6. J. Szklarzewicz, A. Jurowska, D. Matoga, K. Kruczala, G. Kazek, B. Mordyl, J. Sapa, and M. Papiez. *Polyhedron*, **2020**, *185*, 114589. <https://doi.org/10.1016/j.poly.2020.114589>
7. P. Bera, P. Brandao, G. Mondal, H. Jana, A. Jana, A. Santra, and P. Bera. *Polyhedron*, **2017**, *134*, 230-237. <https://doi.org/10.1016/j.poly.2017.06.024>
8. R. Fekri, M. Salehi, A. Asadi, and M. Kubicki. *Inorg. Chim. Acta*, **2019**, *484*, 245-254. <https://doi.org/10.1016/j.ica.2018.09.022>
9. H.-Y. Qian. *Acta Chim. Slov.*, **2019**, *66*, 995-1001. <https://doi.org/10.17344/acsi.2019.5247>
10. Z.-Q. Sun, S.-F. Yu, X.-L. Xu, X.-Y. Qiu, and S.-J. Liu. *Acta Chim. Slov.*, **2020**, *67*, 1281-1289. <https://doi.org/10.17344/acsi.2020.6236>
11. L.-W. Xue, Y.-J. Han, and X.-Q. Luo. *Acta Chim. Slov.*, **2019**, *66*, 622-628. <https://doi.org/10.17344/acsi.2019.5039>
12. D. A. Paixão, I. M. Marzano, E. H. L. Jaimes, M. Pivatto, D. L. Campos; F. R. Pavan, V. M. Deflon, P. Maia, A. M. da Costa Ferreira, I. A. Uehara, M. J. B. Silva, F. V. Botelho, E. C. Pereira-Maia, S. Guilardi, and W. Guerra. *J. Inorg. Biochem.*, **2017**, *172*, 138-146. <https://doi.org/10.1016/j.jinorgbio.2017.04.024>
13. J. D. Siqueira, S. F. de Pellegrin, S. S. dos Santos, B. A. Iglesias, P. C. Piquini, L. P. Arantes, F. A. Soares, O. A. Chaves, A. Neves, and D. F. Back. *J. Inorg. Biochem.*, **2020**, *204*, 110950. <https://doi.org/10.1016/j.jinorgbio.2019.110950>
14. B. B. Hollo, J. Magyari, S. Armakovic, G. A. Bogdanovic, M. V. Rodic, S. J. Armakovic, J. Molnar, G. Spengler, V. M. Leovac, and K. M. Szecsenyi. *New J. Chem.* **2016**, *40*, 5885-5895. <https://doi.org/10.1039/C6NJ00560H>
15. V. Singh, A. Katiyar, and S. Singh. *J. Coord. Chem.*, **2009**, *62*, 1336-1346. <https://doi.org/10.1080/00958970802546016>
16. H. L. Zhu, J. H. Zhu, C. Chen, Z. Wei, and L. Tian. *Asian J. Chem.*, **2013**, *25*, 8444-8446. <https://doi.org/10.14233/ajchem.2013.14779>
17. Y.-L. Sang, X.-S. Lin, and W.-D. Sun. *Acta Chim. Slov.*, **2020**, *67*, 581-585. <https://doi.org/10.17344/acsi.2019.5595>
18. I. Demir, M. Bayrakci, K. Mutlu, and A. I. Pekacar. *Acta Chim. Slov.*, **2008**, *55*, 120-124. <https://doi.org/10.1353/dss.2008.0061>
19. A. Sousa-Pedrares, N. Camina, J. Romero, M. L. Duran, J. A. Garcia-Vazquez, and A. Sousa. *Polyhedron*, **2008**, *27*, 3391-3397. <https://doi.org/10.1016/j.poly.2008.08.011>
20. Y. Luo, J. Wang, X. Ding, R. Ni, M. Li, T. Yang, J. Wang, C. Jing, and Z. You. *Inorg. Chim. Acta*, **2021**, *516*, 120146. <https://doi.org/10.1016/j.ica.2020.120146>
21. R. A. Gossage and H. A. Jenkins. *Acta Chim. Slov.*, **2009**, *56*, 329-333.

22. P. H. O. Santiago, M. B. Santiago, C. H. G. Martins, and C. C. Gatto. *Inorg. Chim. Acta*, **2020**, *508*, 119632. <https://doi.org/10.1016/j.ica.2020.119632>
23. N. Kitanovski and M. Pockaj. *Acta Chim. Slov.*, **2021**, *68*, 475-482. <https://doi.org/10.17344/acsi.2020.6634>
24. G.-H. Sheng, X. Han, Z. You, H.-H. Li, and H.-L. Zhu. *J. Coord. Chem.*, **2014**, *67*, 1760-1770. <https://doi.org/10.1080/00958972.2014.916795>
25. Y. Huo, Y.-T. Ye, X.-S. Cheng, and Z.-L. You. *Inorg. Chem. Commun.*, **2014**, *45*, 131-134. <https://doi.org/10.1016/j.inoche.2014.04.008>
26. Z. L. You, H. Y. Yu, B. Y. Zheng, C. L. Zhang, C. W. Lv, K. Li, and L. Pan. *Inorg. Chim. Acta*, **2018**, *469*, 44-50. <https://doi.org/10.1016/j.ica.2017.09.011>
27. L. Mazur, K. N. Jarzemska, R. Kaminski, K. Wozniak, E. Pindelska, and M. Zielinska-Pisklak. *Cryst. Growth Des.*, **2014**, *14*, 2263-2281. <https://doi.org/10.1021/cg401866x>
28. Bruker, SMART and SAINT. Madison: Bruker AXS Inc., **2002**.
29. G. M. Sheldrick. SADABS. Göttingen, Germany: University of Göttingen, **1996**.
30. G. M. Sheldrick. *Acta Crystallogr., Sect. C: Struct. Chem.*, **2015**, *71*, 3-8. <https://doi.org/10.1107/S2053229614024218>
31. J. Meletiadis, J. F. Meis, J. W. Mouton, J. P. Donnelly, and P. E. Verweij. *J. Clin. Microbiol.*, **2000**, *38*, 2949-2954. <https://doi.org/10.1128/JCM.38.8.2949-2954.2000>
32. A. A. R. Despaigne, J. G. da Silva, A. C. M. Do Carmo, O. E. Piro, E. E. Castellano, and H. Beraldo. *J. Mol. Struct.*, **2009**, *920*, 97-102. <https://doi.org/10.1016/j.molstruc.2008.10.025>
33. A. A. R. Despaigne, J. G. da Silva, A. C. M. do Carmo, F. Sives, O. E. Piro, E. E. Castellano, and H. Beraldo. *Polyhedron*, **2009**, *28*, 3797-3803. <https://doi.org/10.1016/j.poly.2009.07.059>
34. M. Bakir, R. R. Conry, O. Green, and W. H. Mulder. *J. Coord. Chem.*, **2008**, *61*, 3066-3079. <https://doi.org/10.1080/00958970801993672>
35. A. A. R. Despaigne, J. G. da Silva, A. C. M. do Carmo, F. Sives, O. E. Piro, E. E. Castellano, and H. Beraldo. *Polyhedron*, **2009**, *28*, 3797-3803. <https://doi.org/10.1016/j.poly.2009.07.059>
36. M. Bakir, O. Green, and W. H. Mulder. *J. Mol. Struct.*, **2008**, *873*, 17-28. <https://doi.org/10.1016/j.molstruc.2007.03.001>
37. C. E. Kyriakidis, P. C. Christidis, P. J. Rentzeperis, and I. A. Tossidis. *Z. Kristallogr.*, **1990**, *193*, 261-269. <https://doi.org/10.1524/zkri.1990.193.3-4.261>
38. A. Ray, S. Banerjee, S. Sen, R. J. Butcher, G. M. Rosair, M. T. Garland, and S. Mitra. *Struct. Chem.*, **2008**, *19*, 209-217. <https://doi.org/10.1007/s11224-007-9274-7>
39. C. M. Armstrong, P. V. Bernhardt, P. Chin, and D. R. Richardson. *Eur. J. Inorg. Chem.*, **2003**, 1145-1156. <https://doi.org/10.1002/ejic.200390146>
40. P. Barbazan, R. Carballo, and E. M. Vazquez-Lopez. *CrystEngComm*, **2007**, *9*, 668-675. <https://doi.org/10.1039/b703442c>
41. A. A. R. Despaigne, J. G. da Silva, A. C. M. do Carmo, O. E. Piro, E. E. Castellano, and H. Beraldo. *Inorg. Chim. Acta*, **2009**, *362*, 2117-2122. <https://doi.org/10.1016/j.ica.2008.09.040>
42. B. Samanta, J. Chakraborty, S. Shit, S. R. Batten, P. Jensen, J. D. Masuda, and S. Mitra. *Inorg. Chim. Acta*, **2007**, *360*, 2471-2484. <https://doi.org/10.1016/j.ica.2006.12.019>
43. M. Zhang, D.-M. Xian, H.-H. Li, J.-C. Zhang, and Z.-L. You. *Aust. J. Chem.*, **2012**, *65*, 343-350. <https://doi.org/10.1071/CH11424>
44. Z.-L. You, D.-H. Shi, J.-C. Zhang, Y.-P. Ma, C. Wang, and K. Li. *Inorg. Chim. Acta*, **2012**, *384*, 54-61. <https://doi.org/10.1016/j.ica.2011.11.039>
45. S. Basak, S. Sen, S. Banerjee, S. Mitra, G. Rosair, and M. T. G. Rodriguez. *Polyhedron*, **2007**, *26*, 5104-5112. <https://doi.org/10.1016/j.poly.2007.07.025>
46. S. Das and S. Pal. *J. Mol. Struct.*, **2005**, *753*, 68-79. <https://doi.org/10.1016/j.molstruc.2005.05.037>